

Mapping of the 3D-mass distribution with lensing tomography



Patrick Simon¹, Andy N. Taylor¹ and Jan Hartlap²

¹The Scottish Universities Physics Alliance (SUPA), Institute for Astronomy, School of Physics, University of Edinburgh, Royal Observatory, Blackford Hill, Edinburgh EH9 3HJ, UK

²AIfA, Universität Bonn, Auf dem Hügel 71, 53121, Germany



The Algorithm

Since its detection about a decade ago, weak gravitational lensing – the small, coherent distortions (cosmic shear) of galaxy images (sources) due to the large-scale matter distribution in the cosmos – has become a well-established tool for studying the dark Universe. One conceivable application is the recovery of the cosmic matter distribution giving rise to the cosmic shear signal.

We present a linear algorithm that allows to reconstruct the 3D-distribution of matter based on a lensing survey with redshift information. *All* available redshift information – both accurate source redshifts binned into thin slices and broad redshift information such as wide redshift distributions for faint, high- z source sub-samples – can be combined in a Bayesian sense to find the most likely matter distribution. See Fig. 0 below for the set-up of the problem. The statistical uncertainties of the source redshifts, attached as PDF's of the redshifts to the corresponding source sub-sample, and the statistical uncertainty of the shape measurements can properly be factored into the reconstruction. It is also possible to account for intrinsic alignments of the sources that have an impact on the expected shape noise covariance (its off-diagonal elements), $\mathbf{N} = \langle n_\gamma n_\gamma^\dagger \rangle$, entering the algorithm.

The algorithm – a generalisation of the filter discussed in Hu & Keeton, 2002, Phys. Rev. D., 66, 063506 – is a tunable ($\alpha \in [0, 1]$) Wiener filter, based on the expected signal covariance $\mathbf{S}_\delta = \langle \delta \delta^\dagger \rangle$, of the lensing tomography data

$$\delta = \underbrace{\mathbf{S}_\delta \mathbf{Q}^\dagger \mathbf{P}_{\gamma\kappa}^\dagger}_{\text{step 3}} \underbrace{[\mathbf{N}_d^{-1} \mathbf{P}_{\gamma\kappa} \mathbf{Q} \mathbf{S}_\delta \mathbf{Q}^\dagger \mathbf{P}_{\gamma\kappa}^\dagger + \alpha \mathbf{N}_d^{-1} \mathbf{N}_o + \alpha \mathbf{1}]}_{\text{step 2}} \underbrace{\mathbf{N}_d^{-1} \gamma}_{\text{step 1}},$$

which is numerically computed, step-by-step from right to left, from the vector of the complete gridded shear information, γ , finally yielding the *minimum variance estimate* of the 3D-matter density δ . The noise covariance is split into diagonal and off-diagonal elements, $\mathbf{N} = \mathbf{N}_d + \mathbf{N}_o$. The practical challenge is the large size of all involved vectors and matrices ($\sim (10^5)^2$ elements). Applications of the transformations $\mathbf{P}_{\gamma\kappa}$, \mathbf{S}_δ and \mathbf{N}_o (convolutions) to some vector x are either optimised using a kd-tree or FFT-methods, the implementations of $\mathbf{Q}x$ or $\mathbf{N}_d x$ are trivial. The inverse operator, $[\dots]^{-1}$, is solved iteratively with conjugate gradients.

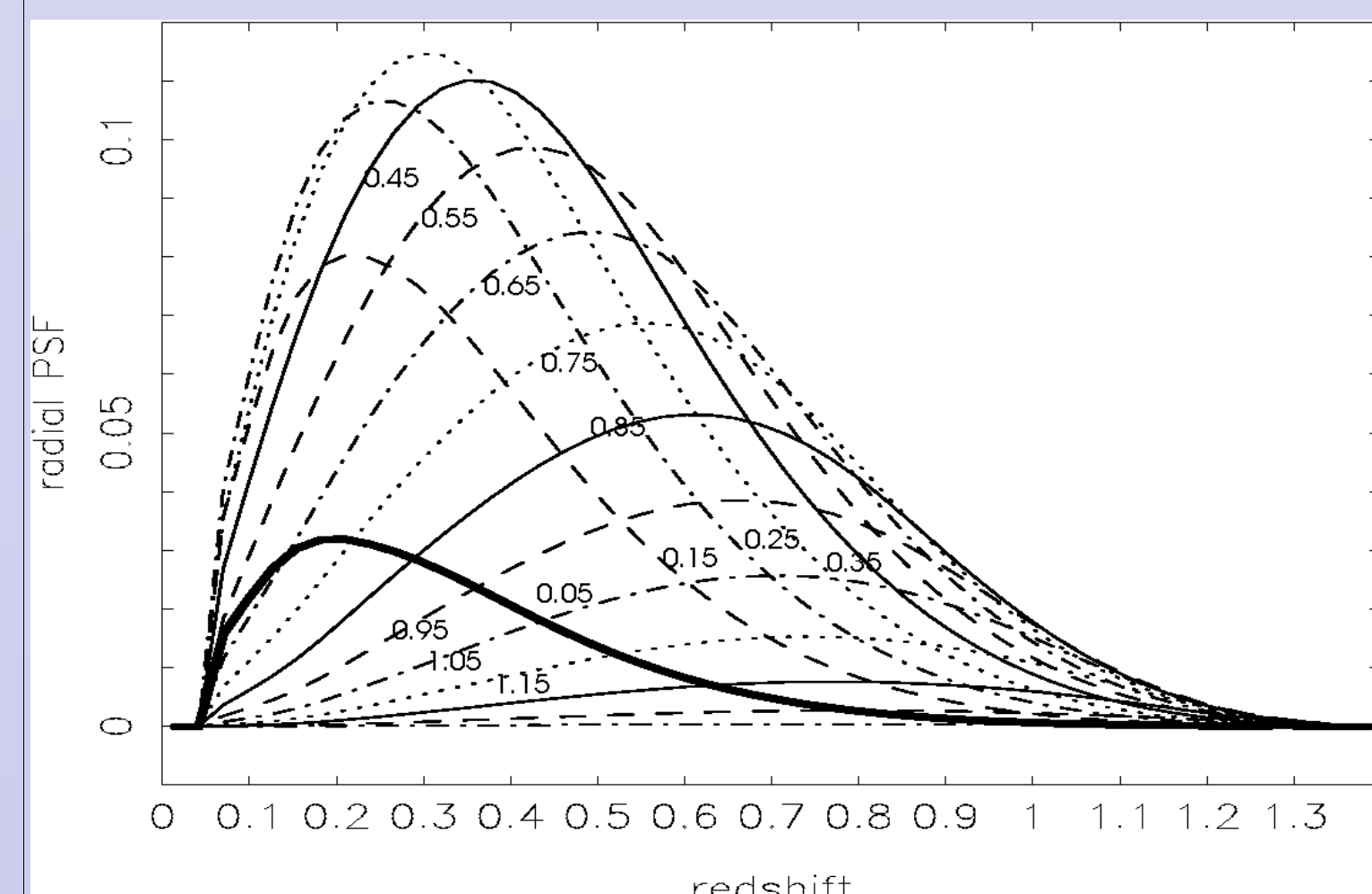


Fig. 2 The radial PSF of a fiducial survey ($\bar{n} = 30 \text{ arcmin}^{-2}$; $\sigma_\epsilon = 0.3$; $\bar{z} = 0.85$, truncated at $z = 1.5$; 15 equally spaced matter slices between $z = 0 \dots 1.5$ and 30 equally spaced source z -slices over same range). A density pixel of radius $1'$ sitting on a lens-plane with certain redshift (numbers attached to curves) is in the process of a reconstruction attenuated and spread out. The figure assumes a transverse Wiener filter with $\alpha = 10^{-2}$. For example, a pixel at $z = 0.05$ is shifted to $z \sim 0.2$ (maximum of PSF) and attenuated with a factor of ~ 0.03 (thick solid line).

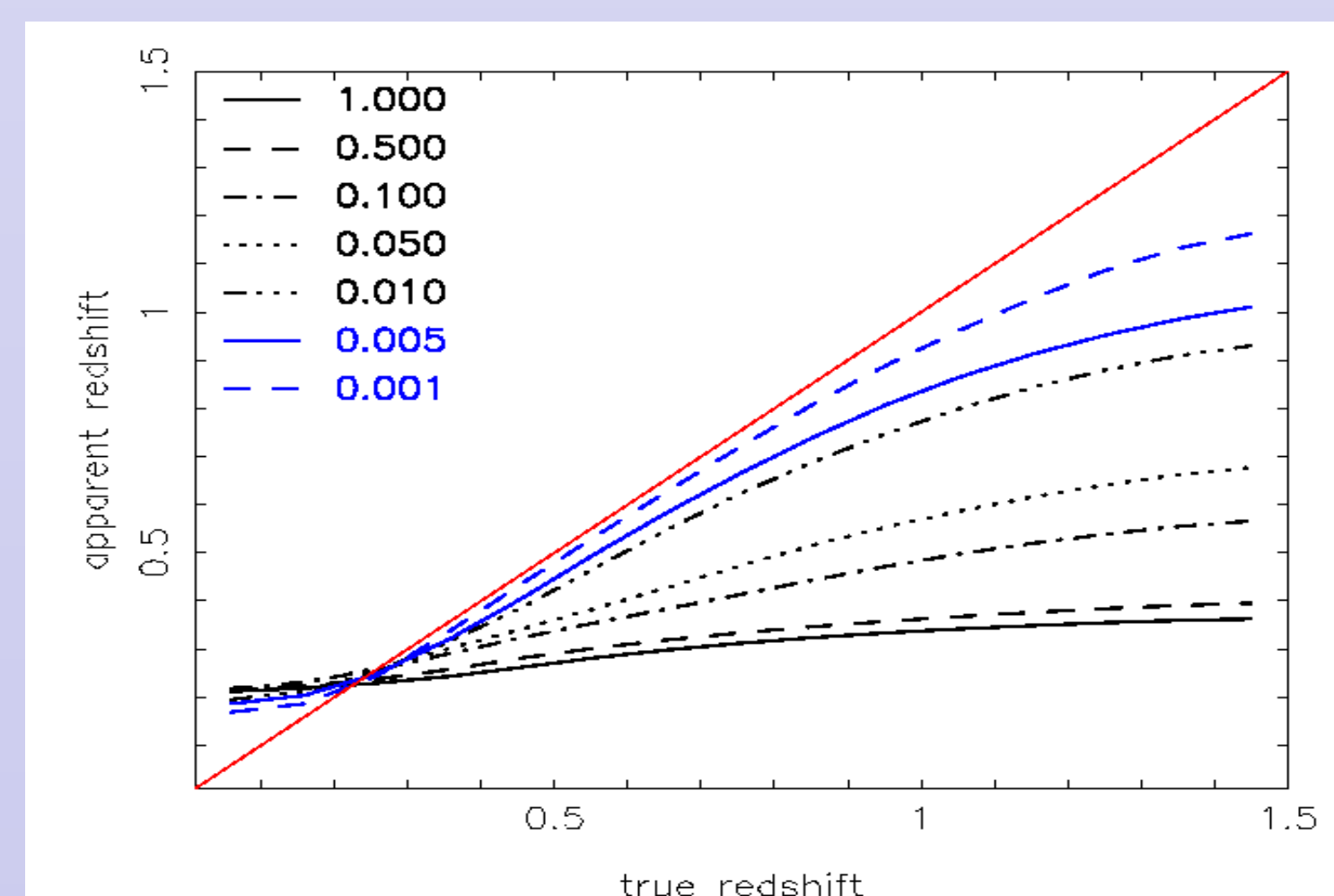


Fig. 3 Shift of peaks in the matter distribution towards wrong redshifts due to Wiener filtering for circular grid-pixels of radius $1'$. The shift depends on the tuning parameter α (different line styles). The same fiducial survey as in Fig. 2 is assumed. To obtain the corresponding plots for different σ'_ϵ or \bar{n}' , but all other parameters kept, one has to rescale $\alpha \mapsto \alpha \times \left(\frac{\sigma'_\epsilon}{\sigma_\epsilon}\right)^2 \left(\frac{\bar{n}}{\bar{n}'}\right)$.

Discussion

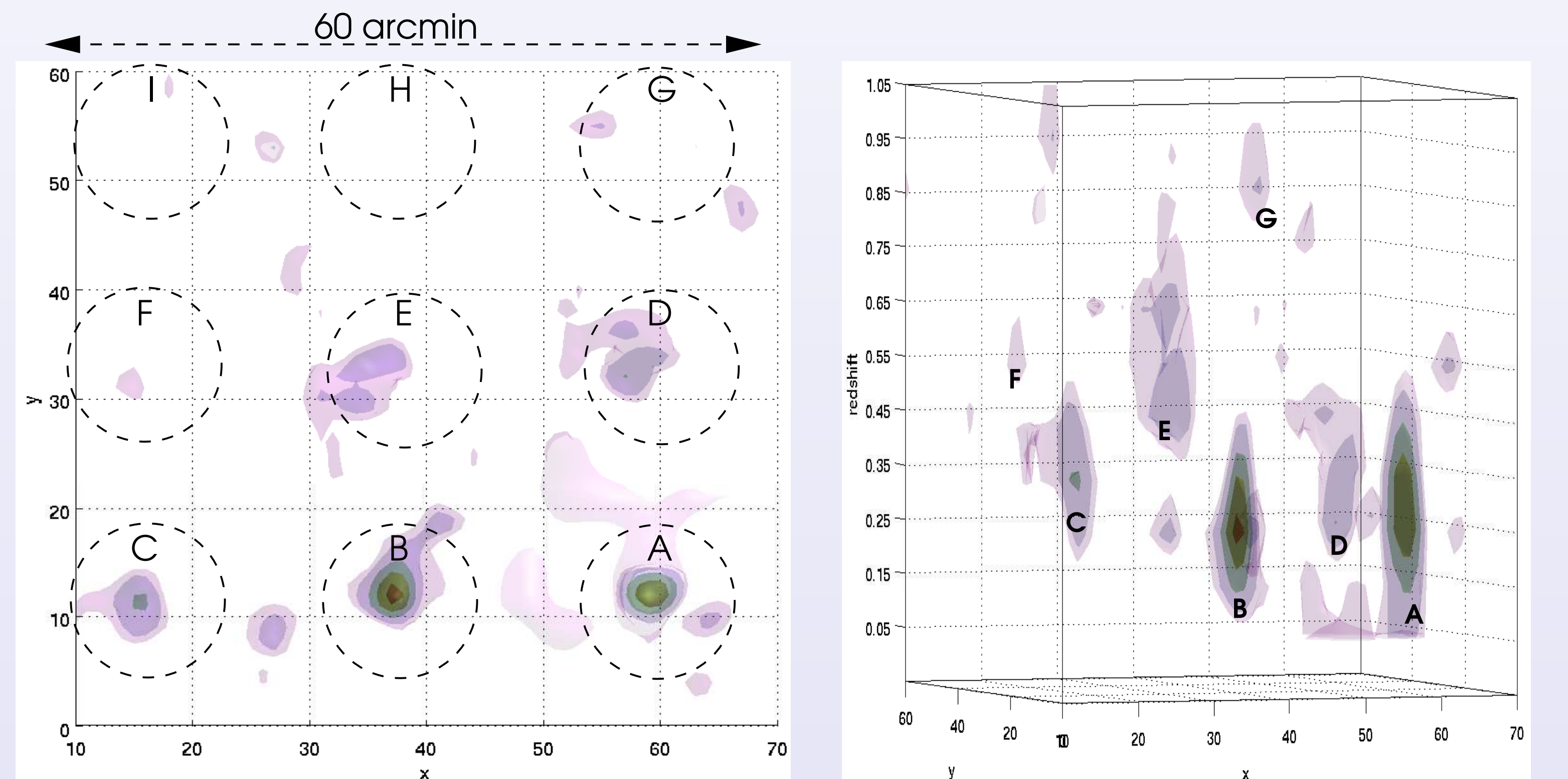


Fig. 1 A set of nine SIS ($\sigma_v = 10^3 \text{ km s}^{-1}$) with redshifts $z = 0.1, 0.2, \dots, 0.9$ (A-I in alphabetical order) is planted into a particular noise realisation of the fiducial survey defined in Fig. 2. The left panel is a 2D-projection of the reconstruction onto the sky, whereas the right panel is a projection showing the extension of the volume in redshift. The differently coloured contours are constant signal-to-noise levels corresponding to $S/N = 8, 6, 5, 3, 2.5$ (darkest to brightest colour). The reconstruction is smoothed on each lens-plane with a Gaussian kernel of radius $1'$. The employed (transverse) Wiener filter has $\alpha = 0.01$. Statistical errors can dissolve peaks as can be seen for D and E or shift peaks towards wrong redshifts, see D for instance.

In practise, due to the relatively small signal-to-noise of shear estimates and the small variations in the weights \mathbf{Q} , signal reconstructions are noisy and biased, i.e. $\langle \delta \rangle$ does not give the original matter distribution. Small or vanishing α 's give extremely noisy, $S/N \sim 10^{-2} - 10^{-3}$, and in radial direction oscillating reconstructions with, however, only little bias. Increasing α , meaning more regularisation, improves the signal-to-noise but smoothes and shifts structures in z -direction, thereby biasing the reconstruction. To lowest order these effects can be described by a radial PSF, Fig. 2. The α has to be tuned to achieve a reasonable pay-off between bias and noise, see Figs. 3 and 4. The bias essentially reflects our inability to pin down exactly the redshift of a density peak due to the noise in the data.

In the extreme case of over-regularisation, one obtains essentially a 2D-reconstruction on the sky, which is stretched out radially over the entire reconstruction range lacking any radial information. A fiducial survey with 30 sources per arcmin^2 , mean redshift of $\bar{z} = 0.85$, $z \leq 1.5$, and $\sigma_\epsilon = 0.3$ is unable ($S/N \lesssim 3$) to identify a matter halo with mass $\sim 10^{15} h^{-1} M_\odot$ or less beyond redshift $z \sim 0.6$ in a reconstruction with moderate ($\alpha \sim 10^{-2}$) z -shift bias, see Fig. 4. The redshift limit increases for deeper surveys. This demonstrates that 3D-mass reconstructions with weak lensing tomography alone are feasible, although probably restricted to massive structures at low or moderate redshifts for near-future surveys.

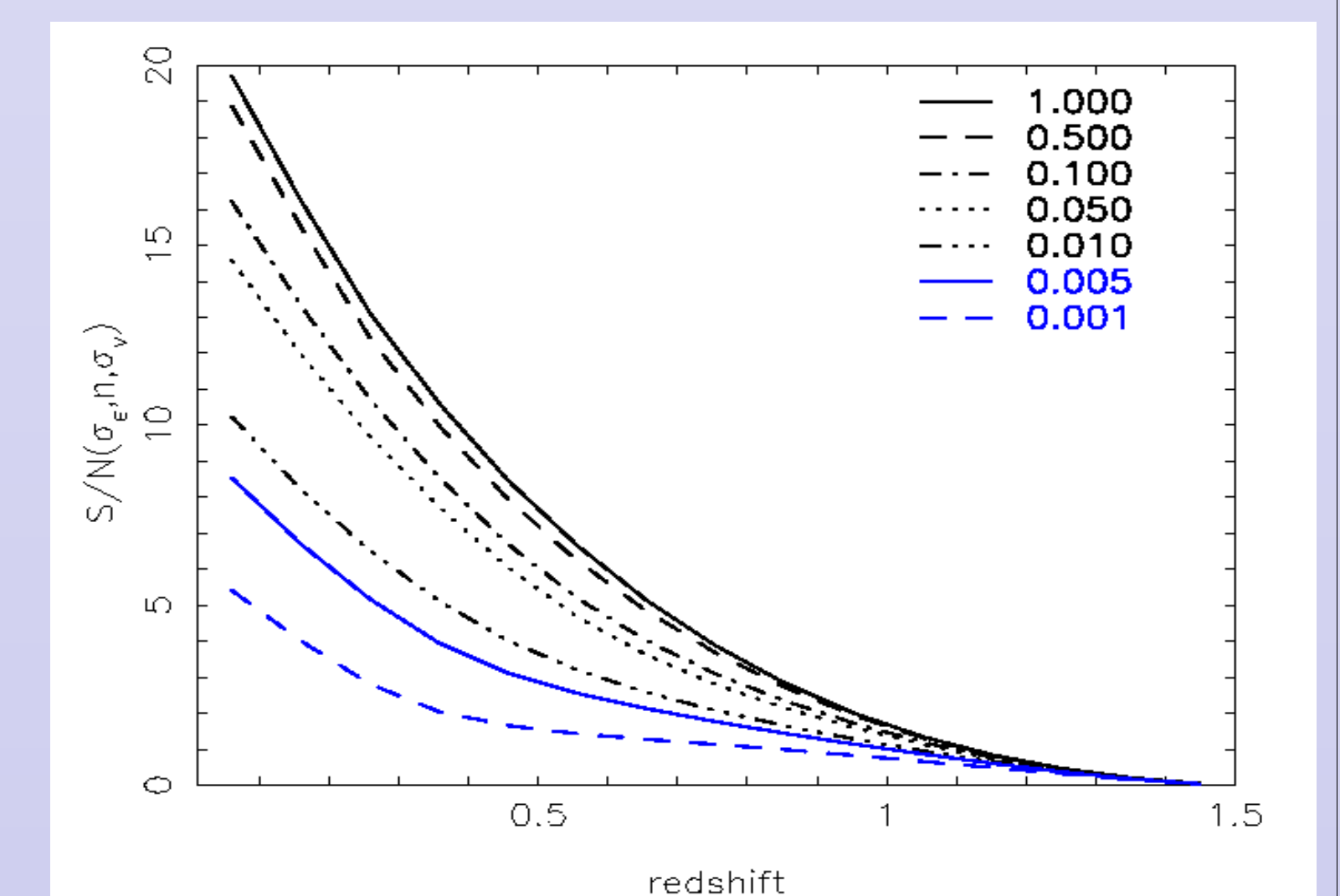


Fig. 4 Signal-to-noise of a reconstructed singular isothermal sphere (central pixel), SIS, positioned at different redshifts, x -axis, with $\sigma_v = 10^3 \text{ km s}^{-1}$; this corresponds to $M_{200} = 6.6 \times 10^{14} M_\odot h^{-1}$ ($1.6 \times 10^{15} M_\odot h^{-1}$) at $z = 0$ (1). Plotted as function of tuning parameter (line styles) the signal-to-noise at maximum response redshift, fiducial parameters as in Fig. 2, the pixel size is $1'$. To obtain the corresponding plots for different σ'_ϵ , σ'_v or \bar{n}' , but all other parameters kept, rescale $\alpha \mapsto \alpha \times \left(\frac{\sigma'_\epsilon}{\sigma_\epsilon}\right)^2 \left(\frac{\bar{n}}{\bar{n}'}\right)$ and $\frac{\bar{z}}{N} \mapsto \frac{\bar{z}}{N} \times \left(\frac{\sigma'_v}{\sigma_v}\right)^2 \left(\frac{\bar{n}}{\bar{n}'}\right)^{1/2}$.

Outline of the Map Making Problem

The (complex) ellipticities of the i th source sub-sample, distinguishable from other sub-samples by the probability distribution (PDF) of source redshifts, are binned on a grid which is covering the survey area. In the weak lensing regime, the gridded ellipticities, $\gamma^{(i)}$, are a weighted sum (2D-projection) of the 3D-matter density contrast thought to be constant within matter slices $j = 1 \dots N_{lp}$. A matter slice is represented by the density contrast $\delta^{(j)}$ on a lens-plane; $\delta^{(j)}$ is binned on the same grid as $\gamma^{(i)}$.

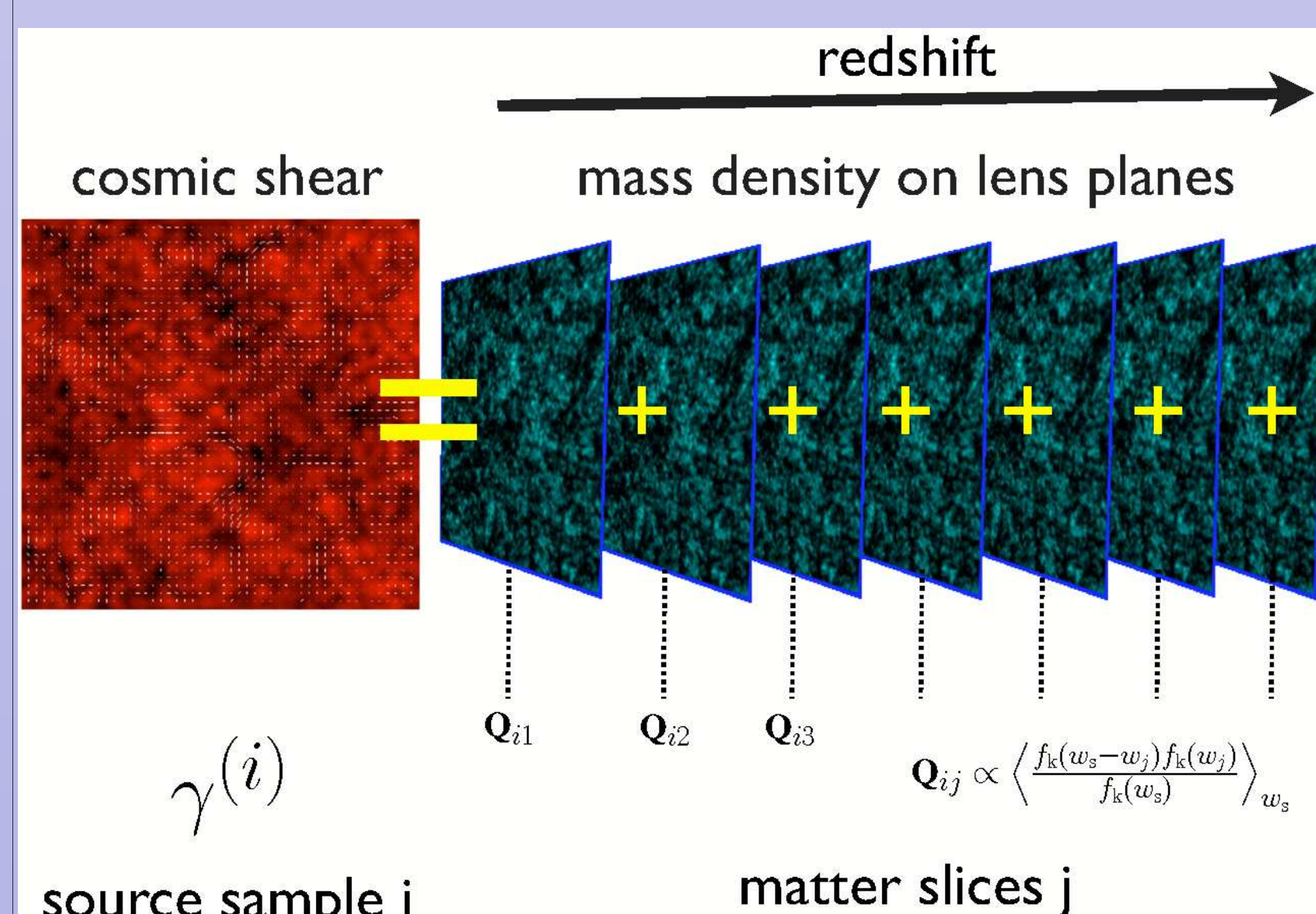


Fig. 0 Illustration of weak lensing being the weighted projection of the 3D-matter distribution.

The weights, \mathbf{Q}_{ij} , are essentially the lensing efficiency averaged over the redshift PDF of i -sources; $f_k(w)$ is the angular diameter distance for a comoving distance w in a given fiducial cosmological model.

For a set of N_s source sub-samples, having distinct source redshift PDF's, we observe the same 3D-matter distribution but projected using different weights:

$$\{\gamma^{(1)}, \dots, \gamma^{(N_s)}\} = \mathbf{P}_{\gamma\kappa} \sum_{i=1}^{N_{lp}} \{Q_{1i} \delta^{(i)}, \dots, Q_{N_s i} \delta^{(i)}\} + \{n_\gamma^{(1)}, \dots, n_\gamma^{(N_s)}\}.$$

Here, $n_\gamma^{(i)}$ denotes the statistical noise that is unavoidably present in the source ellipticities serving as estimator for the cosmic shear signal; it stems from the intrinsic, unlensed shapes of the source images. The convolution $\mathbf{P}_{\gamma\kappa}$ transforms the projected matter density, lensing convergence κ , into the observable cosmic shear γ . As shorthand we can write down this compilation of gridded source ellipticities compactly as $\gamma = \mathbf{P}_{\gamma\kappa} \mathbf{Q} \delta + n_\gamma$. A solution to the map making problem has to invert this equation with respect to the lens-plane matter density δ . This can only be done statistically as the random noise offset n_γ is not explicitly known.